Electrical Life of Vacuum Interrupters for Load Current Switching

Erik D. Taylor, *Member, IEEE*, Martin Eiselt, Ralf Tschiesche, Unni Suresh, and Thomas Brauner

***Abstract*— While the short-circuit current of vacuum interrupters (VIs) is a key performance parameter, very high current operations rarely occur in actual applications. In contrast, switching load and/or capacitive currents comprise virtually all the practical operations. Load current switching requires a low contact erosion and low metal vapor generation of the arc to achieve a long electrical life and is achieved by contacts in vacuum. However, the excellent performance of contacts in vacuum makes the testing and determination of the ultimate electrical life at load currents challenging. Tests on Cu–Cr and Cu–W contacts in VIs were performed at 2500–2700 A rms with 20 000–30 000 switching operations. The VIs with both types of contacts retained their dielectric strength, contact shape and composition, and low contact resistance. Even after arcing operations with total transferred charges >200 kA · s per interrupter, the contacts could continue providing good dielectric and switching performance with low resistance. Contact erosion was minimal and of limited practical significance. These results demonstrate the very long electrical life of VIs when the vacuum arc is naturally diffuse.**

***Index Terms*— Circuit breaker, contact erosion, contactors, load current, vacuum interrupter (VI).**

I. Introduction

VACUUM interrupters (VIs) are a key element of circuit breakers for medium-voltage electrical systems [1] and have increasing applications to high [2] and low voltage [3] systems as well. The outstanding performance of VI was demonstrated early in their development [4], and further efforts have extended the performance and applications of these devices [2]. In terms of the current, applications extend from contactors [5] and load-break switches [1] with maximum interruption currents of some kiloamps to generator circuit breaker applications up to 100 kA rms [6], [7] and specialized applications up to 200 kA [8]–[10] with high reliability [11].

Circuit breaker applications involve two main classifications for the interruption current. The first is the load current, also referred to as normal or continuous current. Load current spans the range from amperes to some thousands of amperes and is seen during the standard operation of electrical power systems. Short-circuit currents, in contrast, lay within the range of thousands of amperes to tens of thousands of amperes. Short-circuit currents appear during events where one or more of the phases are connected to each other and/or to ground.

The end of life for circuit breakers indicates the point beyond which the ability of the breaker to perform its expected duties is impaired (passing current when closed, interrupting load, and short-circuit currents). The mechanical life is the most common practical limit, especially for VI used in contactor and capacitor switching applications [12]. This performance is thoroughly tested in development and type tests.

The next limit would be the number of short-circuit operations. International standards [13] specify an extensive and complex set of short-circuit tests to verify the proper operation of the switch [14]. These standards developed over many years and incorporated extensive practical and theoretical experience [15], [16]. These tests include the verification of performance for terminal faults (where all three phases are short circuited) in power systems with both noneffectively and effectively earthed neutrals [17] and single-phase tests with symmetric [18] and asymmetric currents [19].

The International Electrotechnical Commission (IEC) standard for circuit breakers [13] specifies an electrical endurance test for short-circuit currents referred to as Class E2. This test requires addition tests at 10%, 30%, 60%, and 100% of the rated short-circuit current. Reclosers, which function on overhead lines, also have a test series with operations at 20%, 50%, and 100% of the rated short-circuit current [20]. Another circuit breaker standard specifies 20, 30, or 50 operations at 100% of the rated short-circuit current as an option for Class E2 [21]. However, as mentioned earlier, high short-circuit currents are very rare, and the frequent occurrence of high current, three-phase terminal faults would cause problems in the power systems far beyond concerns over the circuit-breaker lifetime. Nevertheless, considerable evidence exists demonstrating the VI ability to interrupt tens and even a few hundreds of full short-circuit currents [22], [23].

Data on short-circuit occurrences in the field were compiled in [24] and summarized in [14, Sec. 2.4]. Short circuits are generally rare and mostly occur in outdoor systems. Only about 10% of the short circuits involve all three phases, which limits the magnitude of the short-circuit current. The average short-circuit current is less than 20% of the rated value. Therefore, almost all vacuum circuit breakers in service do not approach the end of life based on the short-circuit currents.

Manuscript received 22 December 2021; revised 12 April 2022; accepted 9 May 2022. Date of publication 27 May 2022; date of current version 23 September 2022. The review of this article was arranged by Senior Editor K. W. Struve. *(Corresponding author: Erik D. Taylor.)*

The authors are with Siemens AG, Smart Infrastructure, 13629 Berlin, Germany (e-mail: erik-d.taylor@siemens.com).

Color versions of one or more figures in this article are available at https://doi.org/10.1109/TPS.2022.3175240.

Digital Object Identifier 10.1109/TPS.2022.3175240

Although the interruption of short-circuit currents is a crucial trait of short-circuit breakers, in the vast majority cases, the circuit breaker interrupts load currents.

The final remaining limit for the end of life of circuit breakers would be the electrical life when switching load currents. These are currents seen during the normal operation of the electrical power system. Circuit breakers and recloser standards do not give any specific test procedure for the electrical life at load currents, and only the standard for contactors specifies a procedure in [25, Sec. 7.108]. The test is a function of the utilization category for the contactor, ranging from ac-1 for resistive loads at the rated normal (continuous) current, up to ac-4 with making and breaking currents at six times the normal current for more inductive loads. This standard recognizes the difficulties in performing these tests all the way to the end of life. Instead, enough tests must be performed to allow the reasonable extrapolation of the data to the expected lifetime. The tests can also be performed at any convenient voltage sufficient to maintain the arc voltage. Five or more operations at the end of the test require the correct rated voltage and demonstrate the continued operation of the contactor.

II. End of Life of Vacuum Interrupters

Strong similarity exists between the potential failure modes leading to the end of life between load current and short-circuit switching. Contact erosion is the first mode but is only a practical problem for arcing contacts in air or oil. For example, the volume erosion rate of Ag–W contacts in air at 12 kA rms [26] is 12 times the erosion of Cu–Cr contacts at 12.5 kA rms in a vacuum circuit breaker [22]. The erosion of contacts in oil at 1000 A rms is 27 times the erosion of contacts in vacuum under similar conditions [27]. Ag–W and Cu contacts in air are also compared to butt contacts of Cu in vacuum over a wide range of currents in [1, Fig. 2.42] and again show the much lower erosion of contacts in vacuum up to peak currents of ∼20 kA. Contact erosion in vacuum exists, and there are measurements of the values [22], [23], [28], [29]; however, it is of little significance for practical applications and plays a role only in arc furnace [30] and tap changer applications [27].

The loss of the contact shape and/or mechanical integrity is the next failure mode. Contacts can lose the original contact shape during arcing, and this loss can lead to the end of life of the interrupter through the loss of magnetic arc control [31], [32]. In addition, the contact melting during arcing and resolidification can damage the contacts. This is especially a problem for arcing in air [33], [34].

Losing the dielectric strength of the interrupter serves as the third failure mode. Two main sources for VI are damage to the contact surface leading to an increase in the electrical field and metal vapor deposit on ceramic surfaces [35]. Melting during the arcing process sets the amount of the contact damage, while the internal structure of the VI, particularly of the shields around the arcing chamber controls the amount of metal vapor that deposits on the ceramics [36].

The increase in contact resistance is the final mode. Excessive resistance increase can cause the temperature rise of the circuit breaker to exceed the accepted limits for load current flowing through the closed contacts. Contacts in air face this problem because of oxidation of the contact surface from arcing [33]. Vacuum does not face this problem, and the resistance increase is confined to changes in the contact surface [37]. These four potential failure modes derive from contact erosion and its effects on the VI performance.

The behavior of the vacuum arc and the arc control techniques used in VIs enable the extraordinary long electrical life both at load and short-circuit currents. There are three main contact structures. The first is a simple butt contact. Applications of the butt contact are normally restricted to contactors and load break switches, where the maximum interruption current is limited to 4–10 kA rms. Up to the lower end of this current boundary, the vacuum arc is naturally diffuse and burns over all or most of the contact surface. In the peak current range of 6–15 kA, the arc on butt contacts burns in the diffuse column mode, with arcing spread over the surface of the contacts but with a concentration of cathode spots in one region [38]. This concentration leads to lightly melted craters on the contact surface and likely an increase in the erosion rate compared to the diffuse arc mode. Above peak currents of 15 kA, the arc on butt contacts converts into a constricted arc, with a rapidly increasing erosion rate [39].

Arc control techniques are generally required when the peak current is above 15 kA and sometimes are also used applications with peak currents between 6 and 15 kA. The two main arc control techniques use the magnetic field generated by the short circuit to control the arc behavior [40]. These techniques either generate an axial magnetic field (AMF) between the contacts to maintain a diffuse arc at high currents or a radial magnetic field (RMF) that forces the arc to rotate on the contact surface. With both designs, the arc remains naturally diffuse up to peak currents of 6 kA, and the arc control begins to play a significant role only at higher currents. The vacuum arc becomes diffuse as the current decreases toward the current zero (CZ) before interruption [38].

Earlier experiments on the vacuum electrical life studied short-circuit current for Cu–Cr contacts [22], [23] and currents from 450 to 600 A rms for Cu–Cr and Ag–WC contacts [28], [29]. Currents of 450–600 A rms are typical of the load current switching in VI, and these studies measured the contact erosion and the sources. Measurements on Cu–W at 600 A rms studied the erosion rate and the contact mechanical integrity [41]. Ernst *et al*. [35] briefly described the dielectric behavior of VI after 10 000 switching operations at 1250 A rms. This work focuses on studying the electrical life at load currents of two VI with different contact materials, particularly looking at all four potential failure modes that result in an end of the electrical life.

III. Experimental Description

Tests were performed on two different types of VIs. Both tests used three VI installed into a commercial circuit breaker for Cu–Cr contacts or a commercial contactor for Cu–W contacts. Three-phase currents of 50 Hz for close-open (C-O) in a noneffectively earthed circuit were used for the switching

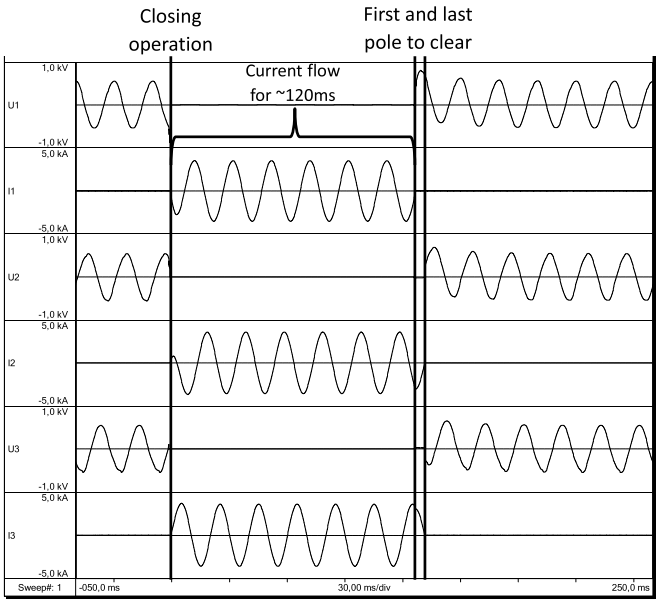

Fig. 1. C-O operation on Cu–Cr contacts for a three-phase current of 2500 A rms. Figure plots the voltages and currents of each phase. Current begins to flow after the close operation (indicated vertical line) and is interrupted in the first phase to clear and then 5 ms later in the second and third phases to clear.

operations. Current flow of 120 ms was initiated by the contact closing operation. The switch then opened the contacts, started the arcing, and then interrupted the current. Both the contact closing and opening operations were not coordinated with the phase of the test current. This would be expected to give a random distribution of the opening and closing times. Fig. 1 shows an example of one C-O operation.

Because a three-phase ungrounded circuit was used for testing, one VI would interrupt the current first and become the first phase to clear. The other two phases were then in series and would have a CZ 5 ms after the first phase to clear. One phase would have its CZ delayed compared to a standard 50 Hz cycle. This phase has a higher transferred charge and is referred to as the second phase to clear. The other phase would have a shorter arc time than expected and is the third phase to clear [14].

The C-O operations occurred at a rate of one operation per minute. The current and arcing time of each phase was measured during each operation, allowing for the calculation of the transferred charge. The power frequency withstand voltage U_d [42] was measured periodically during the test sequence. For the Cu–Cr contacts, the lightning impulse withstand voltage U_p [42] was also measured. The voltage insulation of the test switches limited the voltage that could be applied during the test. At the end of the tests, the VI was removed from the switches and the voltage tests were repeated at the maximum values. The contact resistance over the VI was measured at the beginning and end of the tests.

Tests on Cu–Cr contacts used 58-mm-diameter spiral contacts, which produce RMF arc control. The particular VI style used provided good shielding of the ceramic from the metal vapor during arcing. The VI was tested in an air-insulated

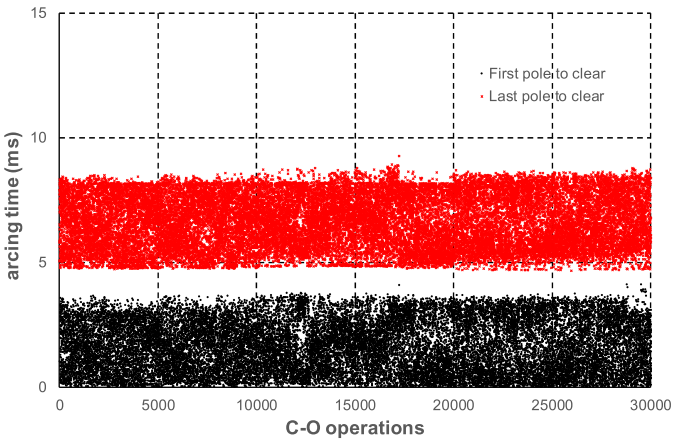

Fig. 2. Arcing times for Cu–Cr contacts as function of operation number. Times for the first phase to clear indicate interruption at the first CZ, with the interruption on the second and third phases ~5 ms later.

circuit breaker used for $U_r = 12$ kV rms rated voltage [13] applications with a rated normal current I_r [13] of 2500 A rms. The VI is also used for $U_r = 24$ kV rms applications with additional external insulation. The test circuit was 690 V rms for 2500 A rms at 50 Hz with an average power factor of $\cos\varphi = 0.78$. A total of 30 000 C-O operations were performed.

The tests on Cu–W contacts used 24-mm-diameter butt contacts. The shielding around the contacts protected the ceramic less than in the Cu–Cr case. The VI was tested in an air-insulated contactor used for $U_r = 12$ kVrms applications and a rated operational current I_e [25] of 450 A rms. The test circuit was 420 V rms at 50 Hz and an average power factor of $\cos\varphi = 0.31$. For contactors, [25, Sec. 6.107] gives a procedure for electrical life testing that was followed here. The contactor was tested according to the ac-4 procedure, with the making and breaking current equal to six times I_e for 2700 A rms. After 10 000 and 20 000 operations, five C-O operations were performed at the full rated voltage of 12 kV rms and current of 2700 A rms.

IV. Experimental Results for Cu–Cr Contacts

Fig. 2 plots the arcing time of the first and last phases to clear. The two bands for the arcing times demonstrate that the circuit breaker reliably stopped the current at the first possible zero crossing of the current (CZ). The first CZ for 50 Hz occurred between 0 and 3.3 ms. The second and third phases to clear then interrupt at the following CZ, which happened at 5.0–8.3 ms. The data sat within these bands with only minor deviations. Although the voltage was below the rated U_r, failures to interrupt can occur at surprisingly low recovery voltages when the performance limit is exceeded [43]. This provided the initial evidence that the performance of the VI is not degraded during the switching operations.

Fig. 3 shows the cumulative transferred charge $\sum Q_{\text{phase,op}}$ during arcing for each phase during the C-O operations. The transferred charge $Q_{\text{phase},i}$ was calculated for each operation on each phase. $\sum Q_{\text{phase,op}}$ is calculated using the

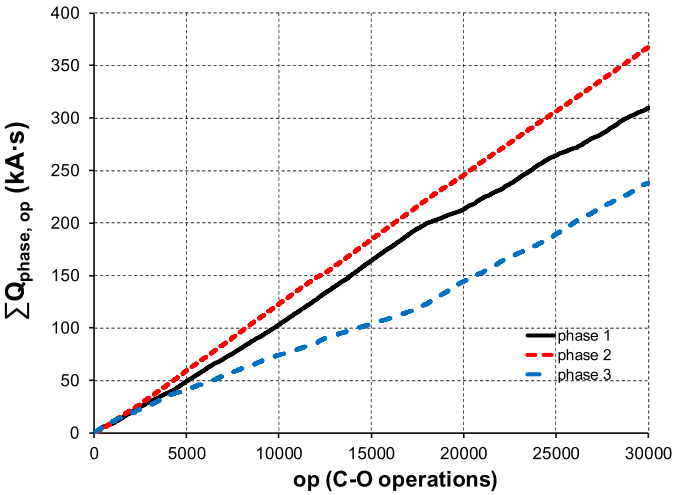

Fig. 3. Cumulative transferred charge during arcing for each phase on Cu–Cr contacts (1) plotted against the operation number.

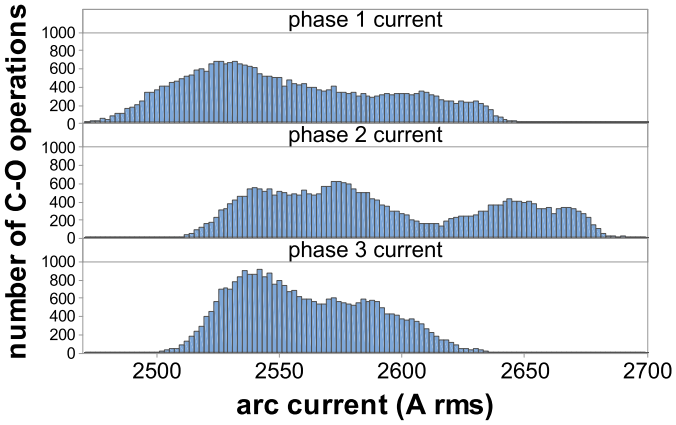

Fig. 4. Histogram of the number of operations with a given current for Cu–Cr contacts, plotted for each phase.

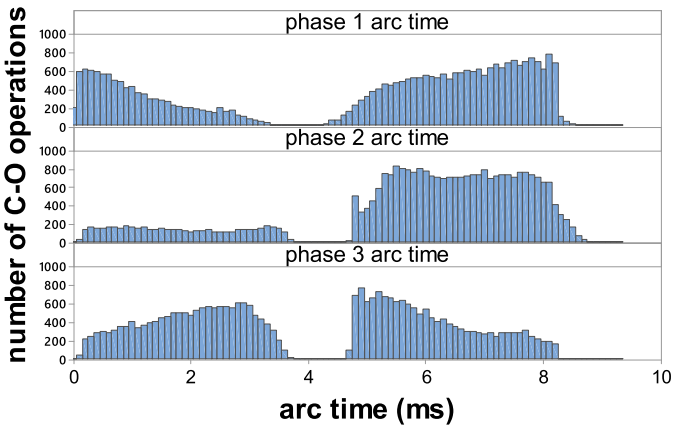

Fig. 5. Data from Fig. 2 replotted as a histogram of the number of operations with a given arcing time for Cu–Cr contacts, plotted for each phase.

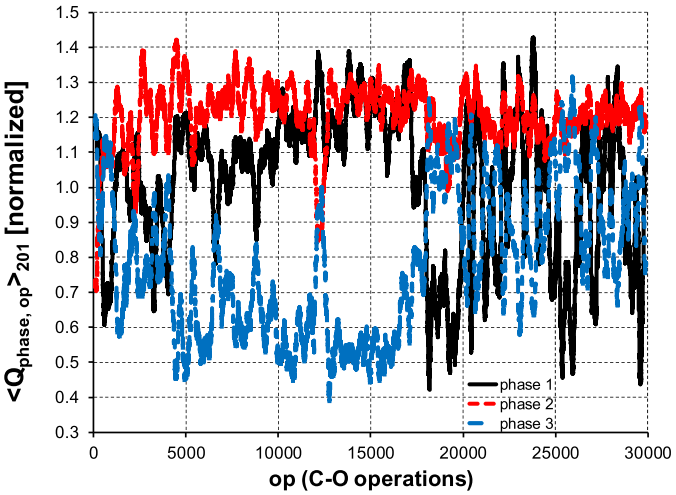

Fig. 6. Moving average of the transferred charge for Cu–Cr contacts [(3) with $n = 201$] for each phase as a function of the number of operations.

following equation:

$$\sum Q_{\text{phase,op}} = \sum_{i=1}^{\text{op}} Q_{\text{phase},i} \tag{1}$$

where i is the specific operation number. All three phases had increasing transferred charge with the number of operations, with the expected general linear rate.

However, there are nontrivial differences in $\sum Q_{\text{phase,op}}$ between the phases. Phase 2 had the most transferred charge, followed by phases 1 and 3. During the testing, no clear difference was noticed. Only at the completion of the test were the distributions of the current shown in Fig. 4 and the arcing time shown in Fig. 5 available. Fig. 4 shows the distributions of the arcing current over the three phases. The distribution for phase 2 was shifted to higher currents and therefore would lead to a larger $\sum Q_{2,\text{op}}$. Fig. 5 shows the distribution of the arcing times over the three phases. Here, phase 3 had its distribution of arcing times shifted to lower values, which would lower $\sum Q_{3,\text{op}}$.

Calculating the moving average of the transferred charge simplifies the comparison between the phases. The calculation first determines $\langle Q \rangle$ the average transferred charge per operation, using

$$\langle Q \rangle = \frac{1}{3 \cdot N} \sum_{\text{phase}=1}^{3} \sum_{i=1}^{N} Q_{\text{phase},i} \tag{2}$$

where N is the total number of operations. The moving average $\langle Q_{\text{phase,op}} \rangle_n$ is calculated using

$$\langle Q_{\text{phase,op}} \rangle_n = \frac{1}{\langle Q \rangle} \cdot \frac{1}{n} \sum_{i=\text{op}-\frac{n-1}{2}}^{\text{op}+\frac{n-1}{2}} Q_{\text{phase},i} \tag{3}$$

where n is an odd number giving the size of moving window over which the data are averaged [44]. When $\langle Q_{\text{phase,op}} \rangle_n = 1$, the moving average is equal to $\langle Q \rangle$.

Fig. 6 plots $\langle Q_{\text{phase,op}} \rangle_{201}$ for the three phases. All three phases have fluctuations in the moving average over the entire test. $\langle Q_{2,\text{op}} \rangle_{201}$ has the highest value throughout the test, while $\langle Q_{1,\text{op}} \rangle_{201}$ and $\langle Q_{3,\text{op}} \rangle_{201}$ switch relative positions. However, $\langle Q_{3,\text{op}} \rangle_{201}$ has a period of $>10\,000$ operations where it is larger than $\langle Q_{3,\text{op}} \rangle_{201}$, and this leads to the higher values for $\sum Q_{1,\text{op}}$

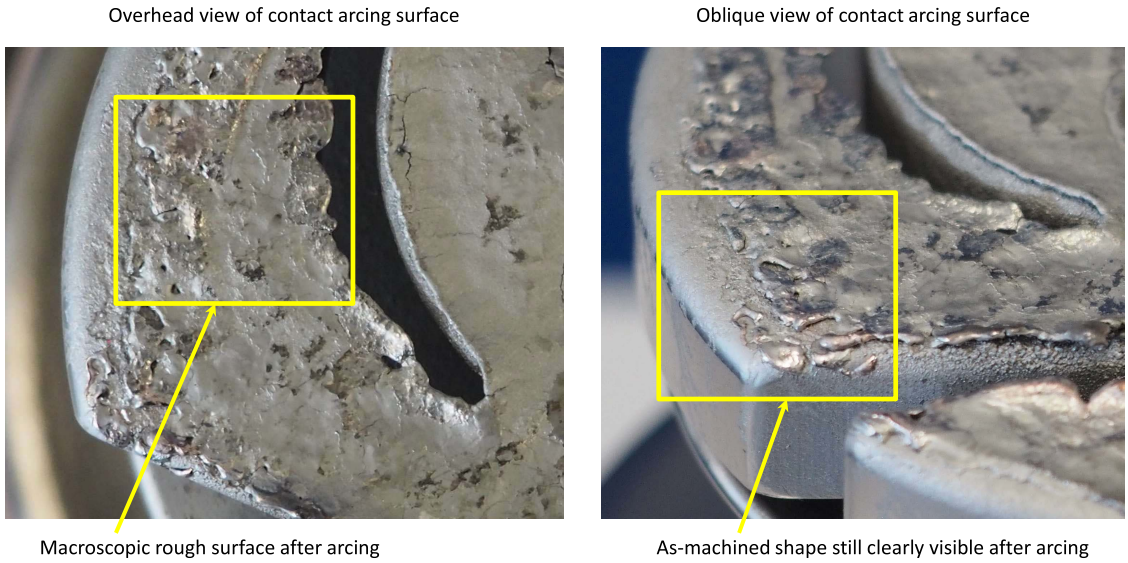

Fig. 7. Photographs of the Cu–Cr contact surface after 30 000 electrical operations.

TABLE I

SUMMARY OF TESTS ON CU–CR CONTACTS. VOLTAGES DURING THE TEST WERE LIMITED BY SWITCH INSULATION. VOLTAGES AFTER THE TEST INCLUDED SUFFICIENT EXTERNAL INSULATION TO ALLOW FULL TESTING OF THE INTERNAL DIELECTRIC BEHAVIOR

Cu-Cr	unit			
<Q>	A·s	10.2		
C-O operations		30 000		
		phase 1	phase 2	phase 3
$\Sigma Q_{phase,\ total}$	kA·s	310	367	238
ΔR	μΩ	2.4	3.5	3.8
ΔR	%	37%	58%	63%
U_d during test	kV rms	42	42	42
U_d after test	kV rms	65	65	65
U_p during test	kV	95	95	95
U_p after test	kV	125	125	125

compared to $\sum Q_{3,\mathrm{op}}$. The value of $n = 201$ was the smallest window that made trends in the transferred charge visible.

Table I summarizes the results for Cu–Cr contacts. After 30 000 operations, $\langle Q \rangle = 10.2$ A · s, while $\sum Q_{\mathrm{phase},N}$ ranged from 238 to 367 kA·s. The VI consistently passed the dielectric tests of $U_d = 42$ kV rms and $U_p = 95$ kV during the tests. These intermediate dielectric values were set by limits in the insulation of the test switch. At the end of the test, dielectric tests on the VI with additional external insulation passed $U_d = 65$ kV rms and $U_p = 125$ kV, meeting or exceeding the requirements of $U_r = 24$ kV rms.

The internal pressure of the VI and the change in resistance over the VI were measured after the complete test sequence. The internal pressure of all three VI was $p \leq 10^{-6}$ hPa and was well within acceptable limits [11]. The increase in the resistance over the VI for the three phases was 37%, 58%, and 63%, respectively. The increase in resistance over the pole of the circuit breaker was 13%, 16%, and 19%, respectively. This increase was well within acceptable limits and would lead to no disadvantage in actual service. The magnitude of these increases is well below the variation in resistance due to connections in the complete switchgear.

Fig. 7 shows the photographs of the contact surface after testing. The contacts in all three VI retained the spiral shape required for arc control including a clear gap between the spiral arms and had not reached the end of life due to the loss of arc control [31], [32]. The contact surface shows a macroscopically rough structure due to the melting and refreezing of the surface from the arcing. However, as noted in Table I, the VI retained their full dielectric performance despite the rough surface. The melted surface constituted only a thin layer, with the as-machined shape of the contacts still readily visible.

The contact erosion rate was calculated by measuring the thickness of the contact pair after arcing. The contacts were aligned to their relative position in the breaker and the thickness compared to the new state. This allowed calculation of the volume change, accounting for the slots in the spiral contacts and other complexities in the contact design. The calculated effective erosion rate was 2.3×10^{-6} cm^3/C. This erosion rate includes both material lost from the contact gap and material pushed off the edge of the contact in the molten state. This effect is visible in Fig. 7. The motion of molten metal off the contact surface has similar consequences as losing material to the center shield and other nearby components.

V. EXPERIMENTAL RESULTS FOR CU–W CONTACTS

Fig. 8 plots the equivalent data as Fig. 2, but for tests on Cu–W contacts; 99.925% of the operations interrupt on the first or second CZ for the first phase to clear and on the next

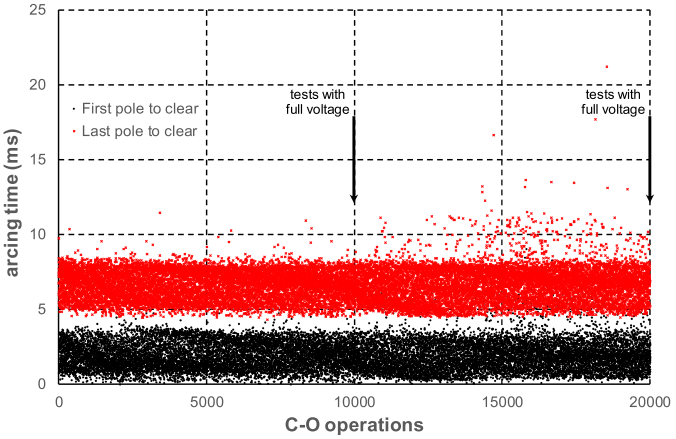

Fig. 8. Arcing times for Cu–W contacts as function of operation number. Times for the first phase to clear indicate interruption at the first CZ, with most interruptions on the second and third phases 5 ms later. Tests with the full rated voltage were performed at 10 000 and 20 000 operations.

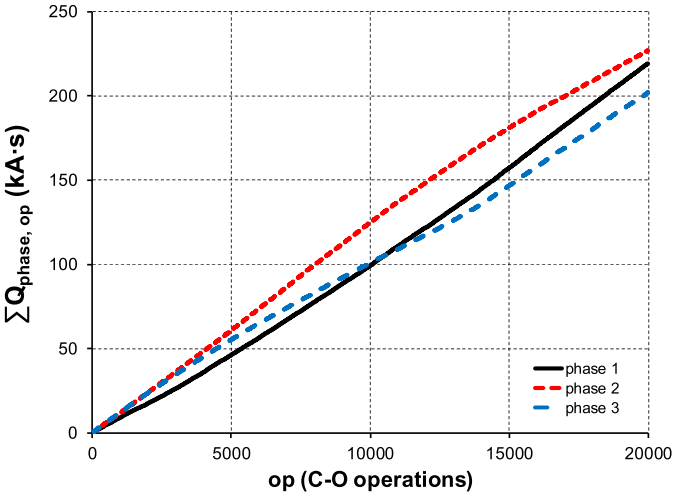

Fig. 9. Cumulative transferred charge during arcing for each phase on Cu–W contacts (1) plotted against the operation number.

possible CZ for the second and third phases to clear, 0.060% of the first phase to clear interrupted on the third CZ, and 0.015% of the second and third phases to clear interrupted on the second possible CZ. This behavior is known from type and development tests on contactors, where a combination of the slow opening speed combined with the lower current interruption performance of the contact materials [1] leads to occasional longer arcing time, but still successful interruption. In addition, after 10 000 and 20 000 operations, five C-O operations were performed at the rated U_r, as specified in [25]. In these tests, 100% of the operations interrupted at the first or second CZ on the first phase to clear and the first possible CZ on the second and third phases to clear.

Fig. 9 plots the cumulative transferred charge $\sum Q_{\text{phase,op}}$ during arcing for each phase during the C-O operations. As with the tests in Section III, all three phases show an increase in the transferred charge with the number of operations, with the expected roughly linear rate. The difference between the phases is not as larger as in Fig. 3. Phase 2 had

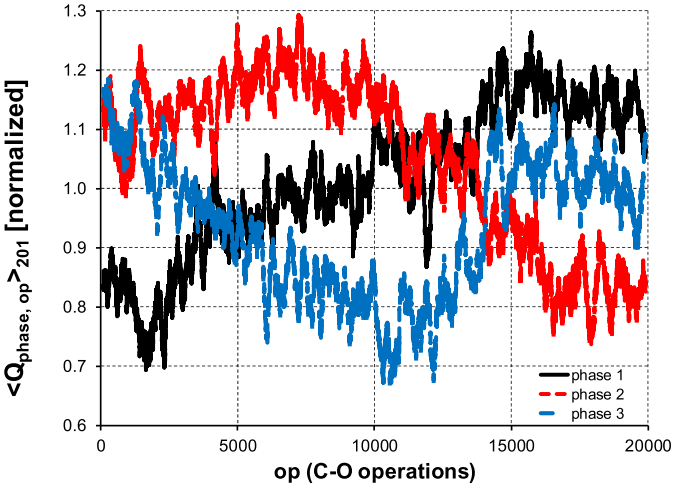

Fig. 10. Moving average of the transferred charge for Cu–W contacts [(3) with $n = 201$] for each phase as a function of the number of operations.

TABLE II

SUMMARY OF TESTS ON CU–W CONTACTS. VOLTAGES DURING THE TEST WERE LIMITED BY SWITCH INSULATION. VOLTAGES AFTER THE TEST INCLUDED SUFFICIENT EXTERNAL INSULATION TO ALLOW FULL TESTING OF THE INTERNAL DIELECTRIC BEHAVIOR

Cu-W	unit			
<Q>	A·s	10.8		
C-O operations		20 000		
		phase 1	phase 2	phase 3
$\Sigma Q_{\text{phase, total}}$	kA·s	219	227	202
ΔR	μΩ	16.5	17.8	0.3
ΔR	%	53%	63%	1%
U_d during test	kV rms	34	34	34
U_d after test	kV rms	42	42	42
U_p after test	kV	45	59	39
U_p after test	%	60%	78%	52%

to most transferred charge, with phases 1 and 3 having similar amounts.

Fig. 10 plots $\langle Q_{\text{phase,op}} \rangle_{201}$ for the three phases. $\langle Q_{2,\text{op}} \rangle_{201}$ has the highest value for most of the first 10 000 operations. Later, the relative position of phase 2 and the other two phases change. However, the earlier buildup of transferred charge produces the $\sum Q_{2,\text{op}}$ behavior seen in Fig. 10. The range of $\langle Q_{\text{phase,op}} \rangle_{201}$ and the fluctuations in value are smaller than for the tests shown in Fig. 6.

Table II summarizes the results for the Cu–W contacts. After 20 000 operations, $\langle Q \rangle = 10.8$ A · s, while $\sum Q_{\text{phase},N}$ ranged from 202 to 227 kA · s. During the test, the VI consistently passed dielectric tests of $U_d = 34$ kV rms (80% of 42 kV rms). These values were limited by the insulation in the test switch. At the end of the test, dielectric tests on the VI alone passed $U_d = 42$ kV rms, which exceeds the

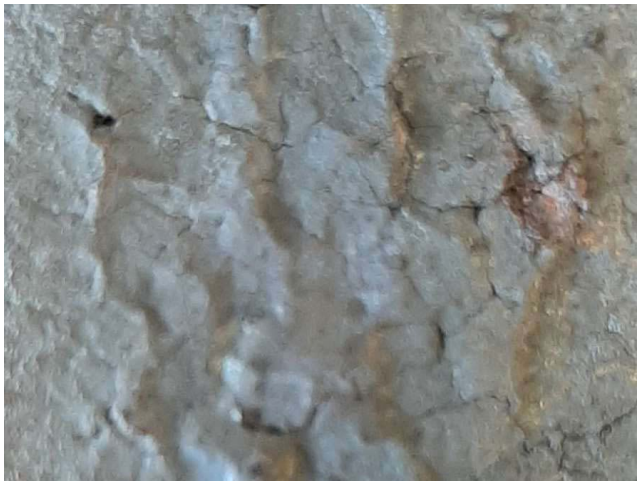

Fig. 11. Photograph of the Cu–W contact surface after 20 000 electrical life operations.

requirements for $U_r = 12$ kV rms [42]. U_p passed 60%, 78%, and 52% of the rated value.

After the testing, internal pressure of the VI and the change in resistance over the VI were also measured. The internal pressure of all three VI was $p \leq 10^{-6}$ hPa and was well within acceptable limits [11]. The increase in the resistance over the VI for the three phases was 53%, 63%, and 1%. The increase in resistance over the pole of the contactor, which includes additional contact joints and current paths, was 17%, 27%, and 0%.

Fig. 11 shows the photographs of the contact surface after testing. The surface is rougher than the Cu–Cr case, and it appears that small (∼0.1 mm height) features are formed over multiple arcing operations and then remelted and mixed with the surrounding contact material in subsequent operations. These features on the arc-facing portion of the contact are small, and the contacts retain their original as-machined shape with only small levels of erosion and deformation. Cathode spots also ran over the sides of the contacts; however, these spots only melted the immediate surface of the contacts.

The erosion rate was also calculated using the same procedure described in Section IV on Cu–Cr contacts. The calculated average erosion rate for Cu–W contacts was 4×10^{-7} cm^3/C. This rate is considerably lower than the already low rate for Cu–Cr contacts and is expected for contacts containing tungsten.

Because of the surface roughness, there were concerns that locally sharp points or edges could lead to higher field emission of electrons and thereby generate X-ray emissions [45]. The X-ray emission from the VI after testing was measured at the U_d values from [42] with a distance of 0.5 m from the center of the VI. When scaled to a distance of 1.0 m using the formula in [42, Sec. 7.11.1.4], the X-ray emissions were ≤ 4 μS/h, which is far below the limit given for new VI in [42, Sec. 7.11] of 150 μS/h at U_d.

VI. Discussion

Electrical life testing at load currents is rarely performed because of the very large number of operations. Performing 30 000 operations at a rate of one operation per minute requires three weeks for the switching time alone. Therefore, evaluating when these results observed here are applicable is very important.

Four potential failure modes for the end of life of VI were discussed in Section II. Contact erosion is the first failure mode. The observed erosion was small and would have little practical relevance. The rates measured here can be compared to the values from [29] for Cu–Cr contacts. The erosion rate is a function of the ratio of the contact gap to the contact diameter, which using the notation of [29] is $g/\langle\varphi\rangle = 0.14$. The measured erosion rate from [29] with this ratio would be 9.1×10^{-7} cm^3/C, which is lower than the value measured here and can be explained by the flow of material off the contact surface while molten. The complex structure of RMF contacts gives more opportunities for material to leave the contact surface, in contrast to simple butt contacts. Nevertheless, the erosion rate remains small and is irrelevant for almost all VI applications.

Loss of the contact shape is the second mode. For Cu–Cr, the thin surface melting has no effect on the overall contact shape and therefore will not result in the overall loss of the arc control. Cu–Cr contacts in vacuum lack the significant damage observed for contacts in air and instead show an uniform melting layer [28], [29], even under dc currents at short-circuit levels [46]. The surface after vacuum arcing is consistent with localized melting of a thin layer by cathode spots, followed by rapid surface resolidification. This maintains some of the surface irregularities from the interaction of the arc pressure and the molten liquid metal [47].

Irregular erosion patterns can appear on Cu–W contacts in vacuum [41], and these patterns are associated with the arc behavior [48]. The arc melting patterns are very similar to those see in [41] at lower currents of 600 A rms. In [41], arcing tests at alternating polarities observed the formation of polycrystalline W particles on the contact surface over multiple arcing operations, which then were remixed with the surrounding contact material in later arcing operations. This led to the formation of small, irregular features on the main arcing surface. The same behavior appeared in these tests. Despite the irregular erosion patterns, the Cu–W contacts retained a very low overall erosion rate and were able to meet the performance requirements of the standards after 20 000 arcing operations and would be expected to continue to perform after even more arcing operations.

The exposure of the insulating ceramic to metal vapor from the arc controls the dielectric performance over the electrical life. The layout of the shield relative to the contact structure controls the amount of resulting ceramic deposit [36]. Maintaining a high level for U_d is very straightforward, and even the basic shield arrangement used in the Cu–W tests was sufficient to maintain $\geq$100% of U_d. Achieving 80% or better of the rated U_d, together with retaining the contact shape and arc control structure, is well proven as a condition check to verify the continued performance of the circuit breaker or contactor [42].

The increase in the contact resistance can be evaluated by comparing it to the values allowed after short-circuit testing in

condition check described in [42, Sec. 7.4.4.2] and the increase in the resistance over the pole of the switch. The increase in resistance for both the Cu–Cr and Cu–W tests was well within the limited set by the condition check in [42] and is similar to the typical increase in resistance after short-circuit testing [37]. The values in the condition check are well established by extensive experience to validate the continued operation of the switch after high-current interruption. The magnitude of the change in the VI resistance is also small when compared to the total resistance in the switch. This demonstrates that the increase in the VI resistance was at most a small perturbation to the overall switchgear resistance and of no concern.

VII. Extension of Results to Higher Currents

The results of this work can be extrapolated to determine what ultimately sets the end of life for load current switching. First, contact erosion is generally not an issue for circuit breaker applications with $I_r \leq 4000$ A rms, where the mechanical life and hence the maximum number of operations at I_r are typically between 2000 and 30 000 operations. Contactors can combine small contact diameters with up to a million mechanical operations; therefore, it is important to estimate the potential erosion to make sure that the loss of contact thickness is kept within acceptable limits. However, this requirement is widely met in practice and very manageable. Applications where $I_r > 4000$ A rms are rare.

AMF VI designs would be expected to maintain a low erosion rate for currents $>$ 4000 A rms based on the continued presence of the diffuse arc mode; however, the erosion rate may be higher than the rates for currents below 4000 A rms. The mobility of the cathode spots is lower in a high-current arc with an AMF than in naturally diffuse arc. This reduced mobility could affect the erosion rate by increasing the local heating, so further research would be useful to measure the exact erosion behavior in arcs in AMF above 4000 A rms.

In RMF systems, the arc is naturally in the diffuse mode up to 4000 A rms, just as for butt contacts. At currents $>$10–15 kA, the arc begins to rotate due to the arc control [31]. Between currents of 6–10 kA, the arc would be in a diffuse column mode. This mode produces shallow, lightly melted craters, where the arc was concentrated [1]. This melting is far less than seen for constricted arcs; nevertheless, the erosion rate would be expected to be higher than for diffuse arc case at $\leq$4000 A rms. RMF VI designs can also be used for $I_r > 4000$ A rms; however, the erosion rate is likely to be higher than for the AMF case. This difference would need to be measured or calculated and then incorporated into the contact design. In general, the method discussed in [22] for extrapolating from the number of full short-circuit interruptions to lower currents is an established and conservative method for estimating the electrical life between the full short-circuit current and $\sim$4000 A rms.

Second, the loss of contact shape can be an issue for small contacts at high currents or for specific contact materials. At some point, it would be expected for small contacts at high currents that the current density would become high enough that these results are no longer applicable. The results here for Cu–W contacts had a peak current density of 8.4 kA/mm^2 and are likely to be applicable to even higher current densities.

These results for the diffuse arc are applicable when the anode contact is passive during the arcing period. An anode spot would significantly increase the contact erosion [1] and thereby increase the possibility for one of the four potential failure modes to occur. All practical VIs are designed to avoid the appearance of the anode spot mode [1], so this limitation is generally not a concern. Only contacts with an unusually large contact gap and particularly small contact diameters see anode spots. Such devices would experience serious problems with current interruption that would be noted during type and development testing.

For contact materials, Cu–Cr gives excellent long-term arcing behavior, with smooth melted surfaces and low erosion. Ag–WC also maintains the contact shape over the erosion tests in [28] and [29]. Cu–W had a more complex melting behavior during arcing and produced some behavior similar to W-based contacts in air [41]. Nevertheless, VI with Cu–W was able to maintain the contact shape necessary for low erosion, small increase in contact resistance, and interruption of the expected currents. The only caveat is Cu–W contact material should not be used for dc currents or other applications where the current does not periodically or randomly switch polarity.

Third, the maintenance of the dielectric strength through the voltage U_d is straightforward, as discussed earlier. In general, if the VI retains good dielectric performance after an electrical life test at short-circuit currents, for example, the Class E2 test in [13], then similar results can be expected for the electrical life at load currents.

Finally, the similarity of the change in contact resistance between short-circuit and load switching operations indicates that if the switch passes the resistance condition check from [42], the contact resistance will not be a limiting factor for the electrical life at load current. This assumes that the contact shape is maintained throughout the electrical life, as changes in the shape beyond those observed in this work could lead to higher increases in the contact resistance.

The differences of the transferred charge between the phases became substantial during the test on Cu–Cr contacts. The differences arose from variation in the arc times between the phases, especially between the number of times the phase is the first versus the second or third phase to clear. Also, small but present differences in the current through the phases also contributed to the variation in transferred charge. The variation between the phases was not apparent over the course of hundreds of operations; the differences only became clear after some thousands of operations. Some possible sources include not quite perfect isolation of the test setup from earth potential and (small) asymmetric placement of the test switch in the setup. No practical electrical system is truly ungrounded; this is the main reason for the clumsy terms in the standards [13], [17], [19] of effectively earthed and noneffectively earthed to describe what a layman would refer to as resistance grounded or ungrounded circuits. Given the rarity of electrical life tests at load current, and the large number of operations required to note variations between the

phases, it is likely that the sources of the variation would be very difficult to eliminate. The experimenter will need to accommodate some difference in the transferred charge between the phases.

VIII. Conclusion

Although a great deal of attention is focused on the short-circuit interruption performance of VIs, the vast majority of switching operations in the field are with load currents. The electrical life at load current is set by the same four factors that determine the electrical life at short-circuit currents. These are the erosion of the contact material, changes in the contact shape, dielectric performance, and change in the contact resistance.

Both Cu–Cr and Cu–W contacts can achieve a long electrical life at load current for load currents $I_r \leq 4000$ A rms. The main point is sizing the contact to maintain acceptable limits on the amount of contact erosion. Typically, erosion will only be a concern for contactors, tap changers, and arc furnace applications with $\gg$30 000 operations. Dielectric performance and changes in contact resistance are generally not limits to the electrical life at load current, if the VI was successful in electrical life tests at short-circuit currents.

The results in this work extend the previous erosion results for electrical contacts in vacuum at 450–600 A rms [22], [23], [28], [29] and dielectric results at 1250 A rms [35]. The higher current of 2500–2700 A rms reproduced the previously seen behavior and verified that all four potential failure modes were absent. Based on the arc mode behavior, which has a key effect on the overall contact erosion rate, the results of this work can be extended up to currents of 4000 A rms. Above this current, the peak current is over 6 kA, and the arc mode can switch to a diffuse column mode with a higher erosion rate. Most medium-voltage circuit breakers have a normal current of $\leq$3150 A rms, with some special applications at 4000 A rms. Applications with $\geq$5000 A rms are generally only seen in special applications like generator breaker applications [6], [7]. Applications above 4000 A rms will have a higher, but still manageable, erosion rate. The exact rate will require further research to measure.

References

[1] P. G. Slade, *The Vacuum Interrupter: Theory, Design, and Application*. New York, NY, USA: CRC Press, 2021.

[2] S. Giere, T. Heinz, A. Lawall, C. Stiehler, E. D. Taylor, and S. Wethekam, "Control of diffuse vacuum arc using axial magnetic fields in commercial high voltage switchgear," *Plasma Phys. Technol.*, vol. 6, no. 1, pp. 19–22, 2019.

[3] H. Fink and R. Renz, "Future trends in vacuum technology applications," in *Proc. 20th Int. Symp. Discharges Elect. Insul. Vac.*, 2002, p. 25.

[4] T. H. Lee, A. Greenwood, D. W. Crouch, and C. H. Titus, "Development of power vacuum interrupters," *Trans. Amer. Inst. Elect. Eng. III, Power App. Syst.*, vol. 81, no. 3, p. 629, 1962.

[5] S. F. Farag and R. G. Bartheld, "Guidelines for the application of vacuum contactors," *IEEE Trans. Ind. Appl.*, vol. IA-22, no. 1, pp. 102–108, Jan. 1986.

[6] D. Gentsch, S. Goettlich, M. Wember, A. Lawall, N. Anger, and E. Taylor, "Interruption performance at frequency 50 or 60 Hz for generator breaker equipped with vacuum interrupters," in *Proc. 26th Int. Symp. Discharges Electr. Insul. Vac. (ISDEIV)*, Sep. 2014, p. 429.

[7] H. Urbanek, K. R. Venna, and N. Anger, "Vacuum circuit breakers—Promising switching technology for pumped storage power plants up to 450 MVA," in *Proc. 4th Int. Conf. Electr. Power Equip.-Switching Technol. (ICEPE-ST)*, Oct. 2017, p. 107.

[8] S. Yanabu, S. Souma, T. Tamagawa, S. Yamashita, and T. Tsutsumi, "Vacuum arc under an axial magnetic field and its interrupting ability," *Proc. Inst. Electr. Eng.*, vol. 126, no. 4, p. 313, Apr. 1979.

[9] T. Bonicelli *et al.*, "The European development of a full scale switching unit for the ITER switching and discharging networks," *Fusion Eng. Des.*, vols. 75–79, pp. 193–200, Nov. 2005.

[10] A. Zamengo, "Operational experience of the 50 kA–35 kV RFX-mod DC-current interruption system," in *Proc. 28th Int. Symp. Discharges Electr. Insul. Vac. (ISDEIV)*, Sep. 2018, p. 543.

[11] E. D. Taylor, A. Lawall, and D. Gentsch, "Long-term vacuum integrity of vacuum interrupters," in *Proc. 26th Int. Symp. Discharges Electr. Insul. Vac. (ISDEIV)*, Sep. 2014, p. 433.

[12] P. G. Slade, W.-P. Li, S. Mayo, R. K. Smith, and E. D. Taylor, "Vacuum interrupter, high reliability component of distribution switches, circuit breakers and contactors," *J. Zhejiang Univ.-Sci. A*, vol. 8, no. 3, pp. 335–342, Mar. 2007.

[13] *High-Voltage Switchgear and Controlgear—Part 100: Alternating-Current Circuit-Breakers*, IEC Standard 62271-100, 3.0 ed., 2021.

[14] R. Smeets, L. Sluis, M. Kapetanovic, D. F. Peelo, and A. Janssen, *Switching in Electrical Transmission and Distribution Systems*. Chichester, U.K.: Wiley, 2015.

[15] G. Lester, "High voltage circuit breaker standards in the USA-past, present, and future," *IEEE Trans. Power App. Syst.*, vol. PAS-93, no. 2, pp. 590–600, Mar. 1974.

[16] *Guide for the Application of IEC 62271-100 and IEC 62271-1 Part 2—Making and Breaking Tests*, Working Group A3.11, Cigre Tech. Brochure 305, CIGRE, Paris, France, Oct. 2006.

[17] E. D. Taylor, J. Oemisch, M. Eiselt, and M. Hinz, "Performance of vacuum interrupters in electrical power systems with an effectively earthed neutral," in *Proc. 27th Int. Symp. Discharges Elect. Insul. Vacuum (ISDEIV)*, 2016, p. 513.

[18] E. D. Taylor, A. Lawall, J. Genzmer, and T. Heydenreich, "Effect of arcing time on the current breaking capability of vacuum interrupters," in *Proc. 2nd Int. Conf. Electr. Power Equip.-Switching Technol. (ICEPE)*, 2013, p. 1.

[19] E. D. Taylor, A. Lawall, and D. Gentsch, "Single-phase short-circuit testing of vacuum interrupters for power systems with an effectively earthed neutral," in *Proc. 28th Int. Symp. Discharges Electr. Insul. Vac. (ISDEIV)*, Sep. 2018, p. 579.

[20] *High-Voltage Switchgear and Controlgear—Part 111: Automatic Circuit Reclosers for Alternating Current Systems Up to and Including 38 kV*, IEC Standard 62271-111/IEEE Standard C37.60, 3.0 ed., 2019.

[21] *High-Voltage Alternating-Current Circuit-Breakers*, GB Standard 1984, 2014.

[22] G. Paul Slade and R. Kirkland Smith, "Electrical switching life of vacuum circuit breaker interrupters," in *Proc. 52nd IEEE Holm Conf. Electr. Contacts*, Sep. 2006, p. 32.

[23] M. Schlaug, L. Dalmazio, U. Ernst, and X. Godechot, "Electrical life of vacuum interrupters," in *Proc. 22nd Int. Symp. Discharges Electr. Insul. Vac.*, 2006, pp. 177–180.

[24] "Life management of circuit-breakers," Working Group 13.08, CIGRE, Paris, France, Tech. Rep. 165, 2000.

[25] *High-Voltage Switchgear and Controlgear—Part 106: Alternating Current Contactors, Contactor-Based Controllers and Motor-Starters*, IEC Standard 62271-106, 2.0 Ed., 2021.

[26] W. R. Wilson, "High-current arc erosion of electrical contact materials," *Trans. AIEE III, Power Apparat. Syst.*, vol. 74, no. 3, p. 657, 1955.

[27] D. Dohnal, *On-Load Tap-Changers for Power Transformers: A Technical Digest*. Regensburg, Germany: Maschinenfabrik Reinhausen, 2009.

[28] M. B. Schulman, P. G. Slade, and J. A. Bindas, "Effective erosion rates for selected contact materials in low-voltage contactors," *IEEE Trans. Compon., Packag., Manuf. Technol. A*, vol. 18, no. 2, pp. 329–333, Jun. 1995.

[29] M. B. Schulman, P. G. Slade, L. D. Loud, and W. Li, "Influence of contact geometry and current on effective erosion of Cu-Cr, Ag-WC, and Ag-Cr vacuum contact materials," *IEEE Trans. Compon. Packag. Technol.*, vol. 22, no. 3, pp. 405–413, Sep. 1999.

[30] A. Greenwood, *Vacuum Switchgear*. London, U.K.: Institution Engineering Technology, 1994.

[31] T. Rettenmaier, "Untersuchung der bewegungscharakteristik von schaltlichtbögen in handelsüblichen vakuumschaltröhren der mittelspannungsebene," Ph.D. dissertation, Fachbereich Elektrotechnik und Informationstechnik, Darmstadt, Germany, 2015.
[32] H. Janssen, V. Hinrichsen, E. D. Taylor, and T. Rettenmaier, "Comparison of arc motion in different lifetime sealed vacuum interrupters with RMF contacts," *IEEE Trans. Plasma Sci.*, vol. 47, no. 8, pp. 3525–3532, Aug. 2019.
[33] C.-H. Leung and H. Kim, "A comparison of Ag/W, Ag/WC, and Ag/Mo electrical contacts," *IEEE Trans. Compon., Hybrids, Manuf. Technol.*, vol. CHMT-7, no. 1, pp. 69–75, Mar. 1984.
[34] P. C. Wingert, "Testing of the thermal-stress-cracking characteristics of silver-refractory contacts," in *Proc. 45th IEEE Holm Conf. Electr. Contacts*, Oct. 1995, p. 338.
[35] U. Ernst, K. Cheng, X. Godechot, and M. Schlaug, "Dielectric performance of vacuum interrupters after switching," in *Proc. 22nd Int. Symp. Discharges Electr. Insul. Vac.*, 2006, pp. 17–20.
[36] A. E. Geisler and N. Wenzel, "Metal vapor deposition in vacuum interrupters: Utilization of DSMC methods and considerations on vapor sources," in *Proc. 28th Int. Symp. Discharges Electr. Insul. Vac. (ISDEIV)*, Sep. 2018, p. 479.
[37] E. D. Taylor, S. A. Baus, and A. Lawall, "Increase in contact resistance of vacuum interrupters after short circuit testing," in *Proc. 27th Int. Conf. Electr. Contacts (ICEC)*, 2014, p. 203.
[38] M. B. Schulman and P. G. Slade, "Sequential modes of drawn vacuum arcs between butt contacts for currents in the 1 kA to 16 kA range," *IEEE Trans. Compon., Packag., Manuf. Technol. A*, vol. 18, no. 2, pp. 417–422, Jun. 1995.
[39] G. R. Mitchell, "High-current vacuum arcs. Part 1: An experimental study," *Proc. Inst. Electr. Engineers*, vol. 117, no. 12, pp. 2315–2326, Dec. 1970.
[40] R. Renz, "Vacuum interrupters," in *Vacuum Electronics: Components and Devices*. Berlin, Germany: Springer, 2008, ch. 8.
[41] P. G. Slade, W. Li, L. D. Loud, and R. E. Haskins, "The unusual electrical erosion of high tungsten content, tungsten copper contacts switching load current in vacuum," *IEEE Trans. Compon. Packag. Technol.*, vol. 24, no. 3, pp. 320–330, Sep. 2001.
[42] *High-Voltage Switchgear and Controlgear—Part 1: Common Specifications for Alternating Current Switchgear and Controlgear*, IEC Standard 62271-1, 2.1 ed., 2021.
[43] E. D. Taylor, A. Lawall, J. Genzmer, and T. Heydenreich, "Current interruption performance of axial and radial magnetic field vacuum interrupters," in *Proc. 28th Int. Symp. Discharges Electr. Insul. Vac. (ISDEIV)*, Sep. 2018, p. 579.
[44] Support.minitab. *Methods and Formulas for Moving Average*. Accessed: Nov. 29, 2021. [Online]. Available: https://support.minitab.com/en-us/minitab/18/help-and-how-to/modeling-statistics/time-series/how-to/moving-average/methods-and-formulas/methods-and-formulas/
[45] S. Giere *et al.*, "X-radiation emission of high-voltage vacuum interrupters: Dose rate control under testing and operating conditions," in *Proc. 28th Int. Symp. Discharges Electr. Insul. Vac. (ISDEIV)*, Sep. 2018, p. 523.
[46] I. Benfatto, A. De Lorenzi, A. Maschio, W. Weigand, H.-P. Timmert, and H. Weyer, "Life tests on vacuum switches breaking 50 kA unidirectional current," *IEEE Trans. Power Del.*, vol. 6, no. 2, pp. 824–832, Apr. 1991.
[47] H. T. C. Kaufmann, W. Hartmann, M. D. Cunha, N. Wenzel, and M. S. Benilov, "Advanced modeling of plasma-cathode interaction in vacuum and low-pressure arcs," in *Proc. 28th Int. Symp. Discharges Electr. Insul. Vac. (ISDEIV)*, Sep. 2018, p. 475.
[48] E. D. Taylor, "Cathode spot behavior on tungsten-copper contacts in vacuum and the effect on erosion," in *Proc. 51st IEEE Holm Conf. Electr. Contacts*, Sep. 2005, p. 135.

Erik D. Taylor (Member, IEEE) received the B.S. degree (Hons.) in applied physics from the California Institute of Technology, Pasadena, CA, USA, in 1993, and the M.S. and Ph.D. degrees in applied physics from Columbia University, New York, NY, USA, in 1995 and 2000, respectively.

In 1999, he joined as a Senior Scientist/Engineer with Eaton Corporation, Horseheads, NY, USA, a Vacuum Interrupter Manufacturer, where he was promoted as a Fellow Engineer in 2004. Since 2008, he has been with Siemens AG, Berlin, Germany, where he is currently a Senior Key Expert in switching technology. He has authored over 80 articles and an inventor on seven patents.

Dr. Taylor is a member of the Current Zero Club and was a Guest Editor for the Special Issue on Vacuum Discharge Plasmas in the IEEE TRANSACTIONS ON PLASMA SCIENCE in 2017.

Martin Eiselt received the Dipl.-Ing. degree in electrical and energy engineering from the University of Applied Sciences, Technische Hochschule Zittau, Zittau, Germany, in 1992.

He is currently the Head of the High Voltage Laboratory, Siemens AG, Berlin, Germany.

Ralf Tschiesche received the Dipl.-Ing. degree in electrical engineering (high voltage engineering) from Technical University Ilmenau (Technische Hochschule Imenau), Ilmenau, Germany, in 1988.

He is currently with the Research and Development Department, specializing in electromagnetic simulations, Siemens AG, Berlin, Germany.

Unni Suresh received the M.Sc. degree specialized in systematic product development from the Technical University of Berlin, Berlin, Germany, in 2008.

Since 2008, he has been with the Research and Development Department, Siemens AG, Berlin, where he is currently a Project Manager for new switching devices.

Thomas Brauner received the Dipl.-Phys. and Ph.D. degrees in physics from Friedrich Schiller University, Jena, Germany, in 2002 and 2007, respectively.

He was with Xtreme Technologies, Göttingen, Germany. In 2008, he joined Osram GmbH, Berlin, Germany, as a Research and Development Engineer for discharge lamps. Since 2013, he has been with Siemens AG, Berlin. His work as Research and Development Project Manager includes the design, manufacturing, and testing of vacuum interrupters.